Stability and electronic structure of the complex K_2PtCl_6-structure hydrides DMH_6 (D=Mg, Ca, Sr; M=Fe, Ru, Os)

S. V. Halilov
Center for Computational Materials Science, Naval Research Laboratory, Washington, DC 20375-5000, USA and Department of Materials Science and Engineering, University of Pennsylvania Philadelphia, Pennsylvania 19104, USA

D. J. Singh*
Center for Computational Materials Science, Naval Research Laboratory, Washington, DC 20375-5000, USA

M. Gupta
Thermodynamique et Physico-Chimie d'Hydrures et Oxydes, EA3547, Batiment 415, Science des Materiaux, Universite Paris-Sud, 91405 Orsay, France

R. Gupta
Service de Recherches de Metallurgie Physique, Commissariat a l'Energie Atomique, Centre d'Etudes de Saclay, 91191 Gif Sur Yvette Cedex, France

(Received 22 June 2004; revised manuscript received 16 August 2004; published 19 November 2004)

The stability and bonding of the ternary complex K_2PtCl_6-structure hydrides is discussed using first principles density functional calculations. The cohesion is dominated by ionic contributions, but ligand field effects are important, and are responsible for the 18-electron rule. Similarities to oxides are discussed in terms of the electronic structure. However, phonon calculations for Sr_2RuH_6 also show differences, particularly in the polarizability of the RuH_6 octahedra. Nevertheless, the yet to be made compounds Pb_2RuH_6 and Be_2FeH_6 are possible ferroelectrics. The electronic structure and magnetic properties of the decomposition product, $FeBe_2$ are reported. Implications of the results for H storage are discussed.

DOI: 10.1103/PhysRevB.70.195117   PACS number(s): 71.20.Lp, 71.20.Be, 61.50.Lt

I. INTRODUCTION

The complex hydrides, DMH_6, D=Mg, Ca, Sr, Eu and M=Fe, Ru, Os form in the cubic ($Fm3m$, No. 225), K_2PtCl_6 structure.[1–6] This structure has D on site 8c $(1/4,1/4,1/4)$, M on 4a (0,0,0), and H on site 24e $(x_H,0,0)$. These compounds are of fundamental interest because of the unusual structural motif and the interest in understanding resulting electronic structure, and the bonding associated with it. Furthermore, they could be of practical interest as potential hydrogen storage materials. Mg_2FeH_6 has very high volume and mass storage efficiency (150 g/l and 5.4 wt. %), but is too stable for reversible room temperature applications.[5,7,8] In this regard, understanding of the electronic structure and cohesion may be helpful in finding modifications that improve the thermodynamics, to produce a material for hydrogen storage in mobile applications.

The crystal structure may be regarded as a cubic double perovskite $A_2BB'H_6$, with $A=D$, $B=M$, and B'=vacancy. Therefore, from a structural point of view, the compounds consist of MH_6 octahedra, well separated by presumably inert D ions, whose role is to fill space and donate charge to the MH_6 units. The cubic $Fm3m$ structure is maintained for all these compounds in spite of large variations of the A and B site cation radii, in contrast to the structural distortions often found in oxide perovskites and double perovskites.

These compounds are insulators, and, like many of the complex hydrides,[5] follow the 18 electron rule, which says that the number of nonbonded metal electrons plus the number of electrons in the metal–ligand bonds should be 18. In the simplest view, this would correspond to full s, p, and d shells associated with the $[MH_6]^{4-}$ structural units. However, Miller and co-workers,[9] have emphasized the importance of ligand field effects in these complex hydrides, and, in fact, the calculated electronic structures for these materials show band gaps within the d manifolds, indicating a more complex situation.[11] In particular, insulating band structures, in qualitative accord with experiment, resulting from band gaps between crystal field split transition metal d manifolds were found in non-self-consistent warped muffin-tin calculations, based on the Xα method with $\alpha=1$.

Here, we reexamine the electronic structures, which we obtain using a full-potential, self-consistent linearized augmented plane-wave (LAPW) method, and use these results, along with calculations of the formation enthalpies, to discuss the bonding of these materials and possible directions for modifying them to alter their stability. In addition we discuss the hypothetical materials, Pb_2RuH_6, which was studied as a potential ferroelectric, and Be_2FeH_6, which is both in relation to ferroelectricity and to better understand their stability.

II. APPROACH

As mentioned, the calculations were done within the local density approximation (LDA) using the general potential linearized augmented planewave (LAPW) method.[12] Local orbital extensions[13] were used to relax the linearization errors

TABLE I. LDA and experimental H positions [x_H(LDA) and x_H(exp), respectively], fully symmetric A_g Raman frequency, $\omega(\mathrm{cm}^{-1})$, and band gap, E_g in eV. a(Å) is the lattice parameter used, which was taken from experiment.

	a	x_H(LDA)	x_H(exp)	ω	E_g
Mg_2FeH_6	6.430	0.2412	0.2420 [2]	1923	1.73 $X-X$
Ca_2FeH_6	7.036	0.2257	0.2300 [4]	1759	1.27 $X-X$
Sr_2FeH_6	7.317	0.2178		1694	1.09 $\Gamma-X$
Mg_2RuH_6	6.629	0.2527	0.2524 [4]	1977	2.93 $X-X$
Ca_2RuH_6	7.229	0.2359		1837	2.29 $X-X$
Sr_2RuH_6	7.600	0.2254	0.223 [1]	1778	2.06 $\Gamma-X$
Sr_2OsH_6	7.626	0.2262		1893	2.26 $\Gamma-X$

for the transition metal d states, and to treat the upper semicore levels of the alkaline earth and transition metal atoms. An LAPW sphere radius $r_H=1.1\ a_0$ was used for H in all the compounds. Metal radii of 1.8 a_0 were used for Mg_2FeH_6 and Ca_2FeH_6. For Sr_2FeH_6, metal radii, $r_{Sr}=2.0\ a_0$ and $r_{Fe}=1.8\ a_0$ were used for Sr and Fe, respectively. For Ca_2RuH_6 and Sr_2RuH_6, metal radii of 1.95 a_0 were used. For Mg_2RuH_6 we used $r_{Mg}=1.8\ a_0$ and $r_{Ru}=1.9\ a_0$. Well converged basis sets, defined by $r_H G_{max}=6.0$, where G_{max} is the plane-wave cutoff were employed. The Brillouin zone sampling during the iteration to self-consistency was done using the special-**k** points method with a $4\times4\times4$ mesh, which corresponds to ten **k** points in the irreducible wedge. Densities of states were generated using a tetrahedron mesh of 145 **k** points in the wedge. Convergence was tested, both for the zone sampling and basis set size, by repeating some calculations with higher $r_H G_{max}=7$ and more **k** points $(8\times8\times8)$. Based on these tests, the present convergence with respect to these parameters is better than 2 mRy/cell for total energies, and better than 1 mRy for band energies.

III. ELECTRONIC STRUCTURE AND THE EIGHTEEN ELECTRON RULE

Crystal field effects, which are important here, may be expected to be sensitive to the H positions. Here we use LDA relaxation to determine the H positions (given in Table I). As may be seen, they are in good agreement with experiment for those compounds for which neutron refinements are available. Table I also gives the full symmetry A_g Raman phonon frequency associated with the H internal structural parameter. Raman and inelastic neutron scattering measurements[14] for Mg_2FeH_6 yield an experimental frequency of 1873 cm^{-1}, in good agreement with the present LDA value of 1923 cm^{-1}. The LDA frequencies follow the reported trend for H bond stretching modes in infrared data,[5] decreasing with increasing D ionic radius, and increasing with increasing M atomic number. It is interesting to note the increase in frequency from Sr_2RuH_6 to Sr_2OsH_6. Generally, the ionic properties of 4d and 5d elements are very similar due to relativistic contraction. The main difference, which is also due to relativistic contraction, is that the s states are lower relative to the d states in the 5d series. This leads to a higher position of the d states relative to ligand states in compounds where the transition elements are cations. The result is reduced covalency. Since covalency softens ionic interactions, the result is a stiffer lattice in 5d ionic compounds relative to the corresponding 4d compounds. A good example is the comparison of $KNbO_3$, which is a good ferroelectric with $KTaO_3$, which has practically the same lattice parameter, but is not ferroelectric.[10]

The calculated electronic band structures are shown in Figs. 1–3. The corresponding electronic densities of states (DOS) are in Figs. 4–6. The electronic structures are qualititively similar to those of Orgaz and Gupta (Ref. 11), in that all the materials are insulating with band gaps within the transition metal d bands.

The band structure for all the compounds studied consists of six H 1s derived bands, holding twelve electrons, followed by crystal field split transition metal d bands. The 1s band width is largest in the Mg compounds, and in the case of Mg_2RuH_6 this is sufficient to yield an overlap between the 1s manifold and the lower d manifold. In the octahedral crystal field of the H, the metal d bands separate into a three-fold degenerate (six electrons) t_{2g} manifold and a two-fold degenerate (four electrons) e_g manifold. The 18 valence electrons then populate the H derived 1s bands and the metal t_{2g} bands; the insulating gap is between the occupied t_{2g} and the unoccupied e_g manifolds. Since these are gaps within a crystal field split d band, LDA band gap errors are expected to be small in the absence of strong correlation effects.[15] However, we note that the gap is between narrow d bands, and so a larger gap may be observed both because of optical dipole selection rules and, in the Fe compounds, correlation effects.

The H 1s character of the lowest six bands may be seen from the projections of the DOS onto the LAPW spheres. The small 1.1 a_0 H spheres, used here, imply that most of the charge of H ions will be outside the sphere. A free H^- ion, stabilized by a Watson sphere (to approximately represent the Madelung field) of radius 3.01 Å, would have only 0.45 e (of 2) inside a sphere of radius 1.1 a_0. In contrast, within the LDA, a non-spin-polarized neutral H atom would have only 0.33 e inside the same sphere.[16] Integrating the H s projection of the DOS over the lowest six bands, we obtain from 0.5 e (Ca_2RuH_6 and Sr_2RuH_6) to 0.52 e (Sr_2FeH_6) inside each H sphere, not far from this simple ionic view especially if one allows for a somewhat different breathing. This is also similar to what was found for $NaAlH_4$.[17] Thus the basic electronic structure is ionic consisting of H anions and D and M cations. These compounds should therefore be viewed as ionic for understanding the crystal cohesion.

However, from the standpoint of understanding the electronic structure and H storage properties, covalency is important. The effects of M—H hybridization are clearly seen in the electronic structures. While the bottom six bands are essentially H 1s bands, they contain the two formally bonding H s–M $e_g\sigma$ combinations (as well as four nonbonding combinations). The lowest band is the symmetric combination of s orbitals, which is a nonbonding combination with M e_g states, but is formally bonding with the nominally unoccupied M s states. This is followed by five more H s bands, including the nonbonding and the formally bonding

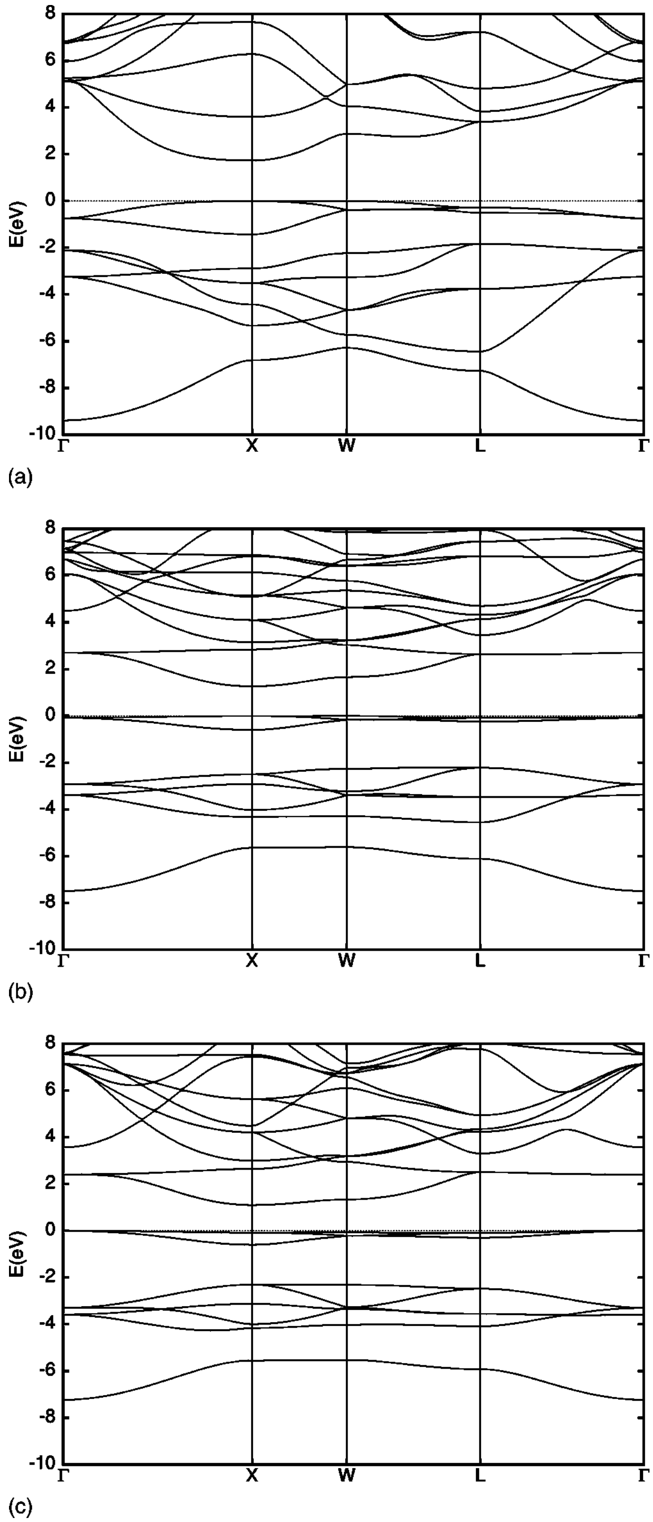

FIG. 1. Band structure of Mg_2FeH_6 (top), Ca_2FeH_6 (middle), and Sr_2FeH_6 (bottom), with the relaxed LDA H positions.

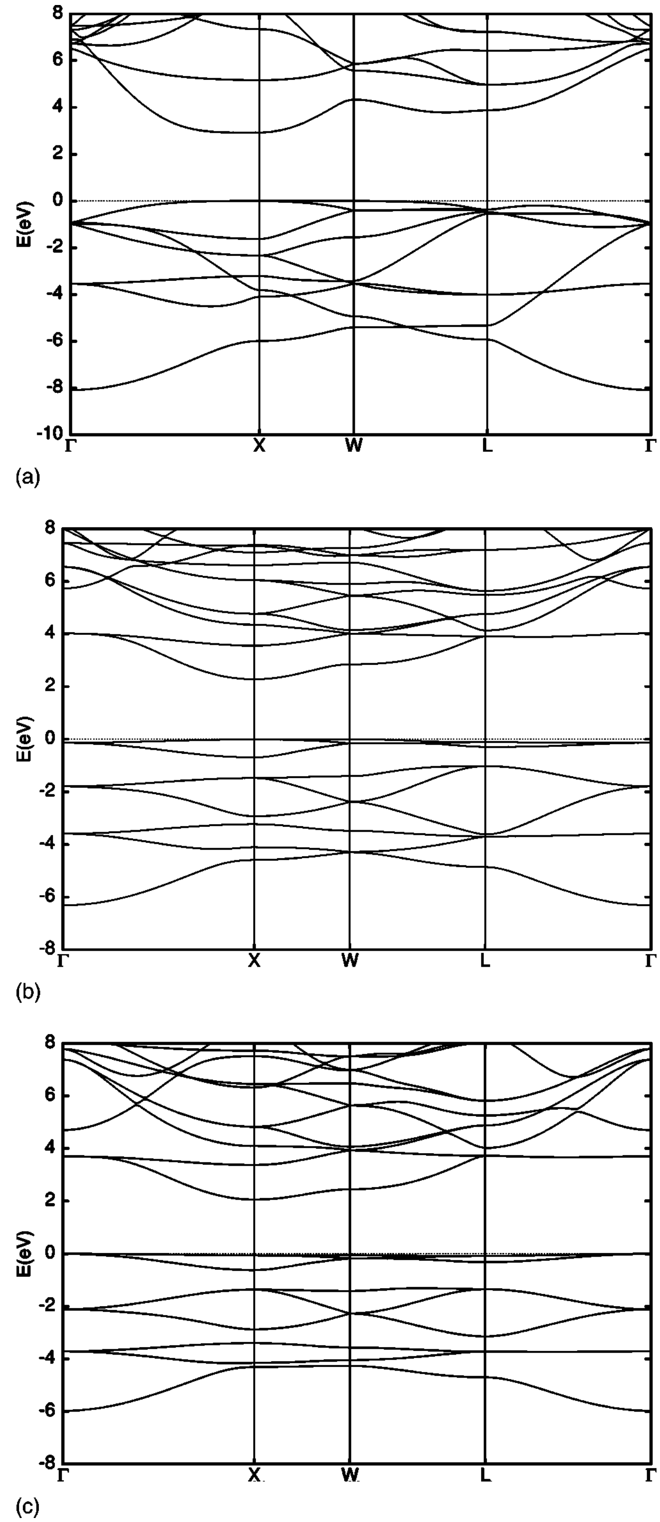

FIG. 2. Band structure of Mg_2RuH_6 (top), Ca_2RuH_6 (middle), and Sr_2RuH_6 (bottom), with the relaxed LDA H positions.

H s–M $e_g\sigma$ combinations. In terms of degeneracies, this division into an "s"-like onefold symmetric band, a fivefold manifold, and the threefold t_{2g} manifold is formally like the s, p, and d electron counting of the 18-electron rule. However, this counting does not correspond to atomic level filling. Instead, the two-electron "s" and ten-electron "d" manifolds are actually from combinations of hydrogen s states, and are therefore very different in atomic character from the six-electron, "p" group, which comes from very weakly hybridized M t_{2g} bands.

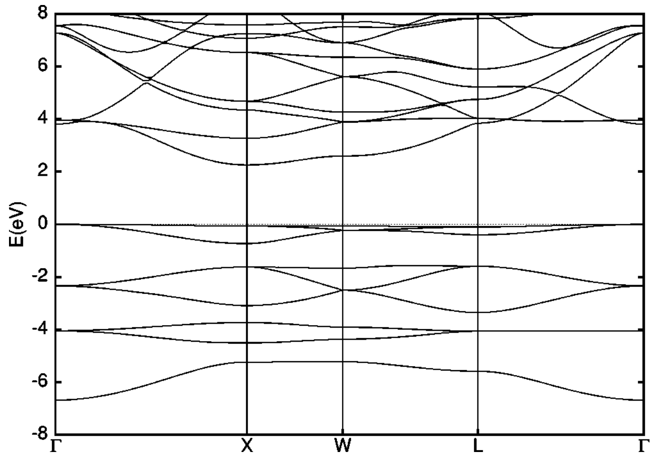

FIG. 3. Band structure of Sr_2OsH_6 with the relaxed LDA H positions.

The lowest conduction bands derive mainly from the corresponding antibonding combinations and *sd* derived states associated with the *D* cation. The covalency in the $[MH_6]^{4-}$ units can be seen in the *M d* contributions to the H *s*, bands for example. The t_{2g} bands show much less hybridization, as expected in an octahedral ligand environment. It should be emphasized that the bands show relatively little dispersion, with the exception of the D=Mg compounds, and that there are generally clean gaps between the different manifolds (H *s*, t_{2g}, and e_g), which implies that weakly interacting $[MH_6]^{4-}$ units may be regarded as the basic building blocks for understanding the band structure. The sizable crystal field splitting of the *M d* bands underlies the 18-electron rule in these compounds. In particular, without it the t_{2g} and e_g manifolds would overlap, and then there would be no barrier to adding more than 18 electrons; the 18 electron rule here is the result of the crystal field splitting of the metal *d* levels. The octahedral geometry, with its large ligand field is energetically favorable for 18 or fewer electrons.[18] The substantial crystal field splittings (as compared to the on-site Hund's coupling, which can be characterized by a Stoner $I \sim 0.7-0.9$ eV for Fe)[19,20] are responsible for the low spin Fe observed in these compounds.

To summarize the results so far, the electronic structure is built up in the following way in decreasing order of the size of the interactions involved. (1) Coulomb interactions, particularly the Madelung field, stabilize an ionic configuration, nominally $D^{2+}M^{4+}H_6^-$. This is the main ingredient in the cohesion. (2) Hybridization between the H *s* orbitals and the $M\ e_g$ orbitals lead to a bonding antibonding splitting between these and contribute to a substantial crystal field splitting between weakly hybridized occupied $M\ t_{2g}$ states and unnoccupied $M\ e_g$ states. This splitting and the position of the *D* derived states well above the t_{2g} energy underlies the 18 electron rule. (3) Hopping between the $[MH_6]^{4-}$ units (presumably mostly assisted hopping via unnoccupied *D s* and *d* states) leads to band formation. This is reminiscent of some of the oxide double perovskites, $A_2MM'O_6$, with an inert M', such as Sr_2RuYO_6, although in that case the hybridization inside the $[RuO_6]^{7-}$ units is very much stronger than in the present hydrides.[21]

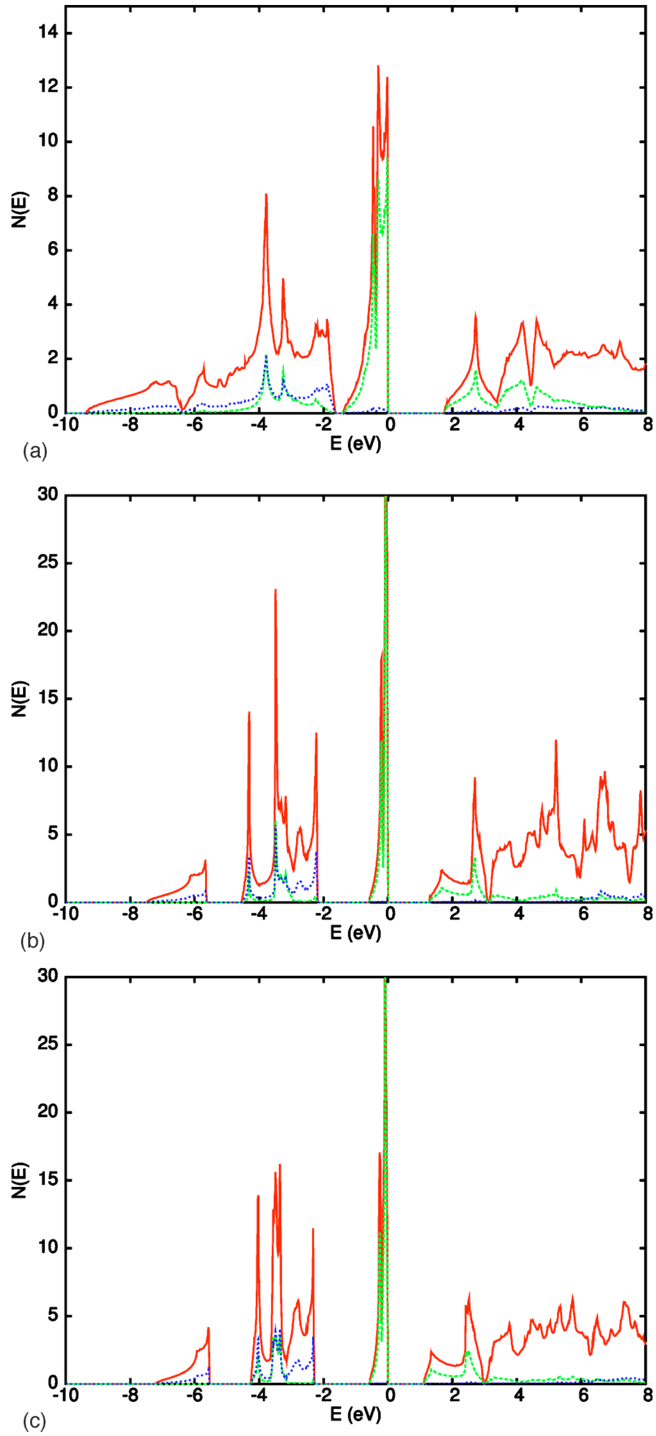

FIG. 4. (Color online) Electronic density of states (heavy red line) and projections onto the LAPW spheres of Fe *d* character (dashed green line) and H *s* character (dotted blue line) for Mg_2FeH_6 (top), Ca_2FeH_6 (middle), and Sr_2FeH_6 (bottom), with the relaxed LDA H positions, on a per formula unit both spins basis.

IV. PHONONS

The resulting image of ionic crystal with substantial covalency between anions and an octahedrally coordinated transition element cation suggests similarities with double perovskite oxides. Furthermore, the fact that the lattice con-

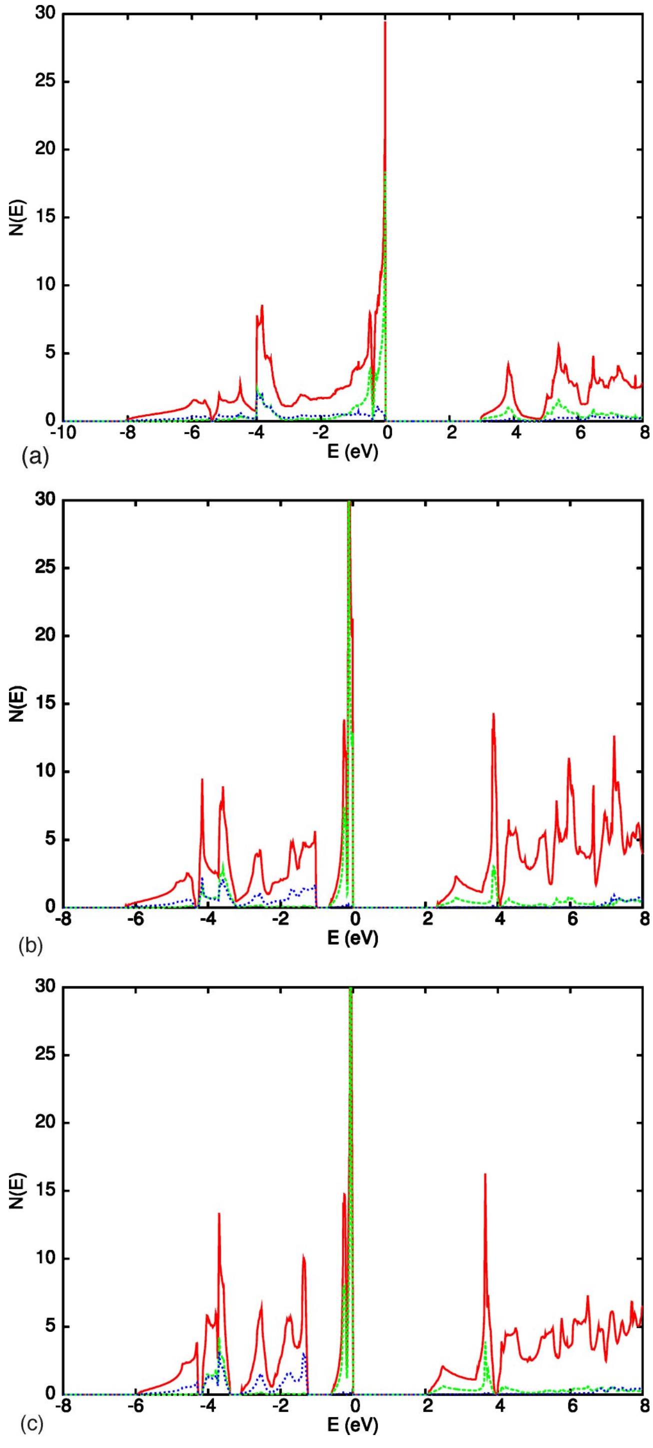

FIG. 5. (Color online) Electronic density of states (heavy red line) and projections onto the LAPW spheres of Ru *d* character (dashed green line) and H *s* character (dotted blue line) for Mg_2RuH_6 (top), Ca_2RuH_6 (middle), and Sr_2RuH_6 (bottom), with the relaxed LDA H positions, on a per formula unit both spins basis.

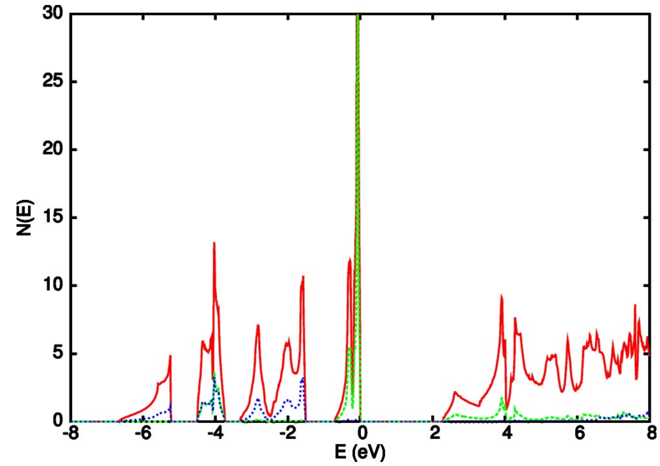

FIG. 6. (Color online) Electronic density of states (heavy red line) and projections onto the LAPW spheres of Os *d* character (dashed green line) and H *s* character (dotted blue line) for Sr_2OsH_6 with the relaxed LDA H positions, on a per formula unit both spins basis.

tains a large anion (H^-) stabilized by the Madelung field and hybridized with nominally unoccupied transition metal states further suggests connections with perovskite oxides, particularly ferroelectrics. In fact, many of the technologically important ferroelectrics are based on perovskites ABO_3 with mixtures of metal atoms on the *B* sites (these can be disordered or ordered as in, e.g., double perovskite). Examples include PZT $[Pb(Zr,Ti)O_3]$, PMN–PT $[Pb(Mg,Nb,Ti)O_3]$, and PZN-PT $[Pb(Zn,Nb,Ti)O_3]$. In these materials both Pb—O and *B*—O hybridization is important in the ferroelectricity.[34]

In order to further elucidate the relationship to oxides, we calculated those zone center phonon frequencies of Sr_2RuH_6 compatible with a rhombohedral *R*32 symmetry, and compare with similar calculations for hypothetical Pb_2RuH_6. This was done at the experimental lattice parameter of Sr_2RuH_6, using the relaxed H position. This noncentrosymmetric group would include the ferroelectric mode, if the material were ferroelectric. The calculations were done by fitting the dynamical matrix to a series of frozen phonon calculations with small displacements of the various atoms. This yields 6 threefold degenerate modes (plus the three $\omega=0$ acoustic modes). The frequencies and displacement patterns of the phonon modes are given in Table II. The 2% difference between the A_g frequencies for Sr_2RuH_6 between Tables I and II reflects the different approaches and should be considered indicative of the errors in the fits used in constructing the dynamical matrix. The fitting errors can also be seen in the deviation of the mode character as given in Table II from the A_g character required by symmetry. For the A_g frequency, the value in Table I should be considered more reliable because that value was obtained enforcing the exact mode symmetry, but it should be kept in mind that the LDA error is likely larger than the difference between the values in Tables I and II.

The highest frequency branches correspond to H motions, as expected. Of these, the A_g Raman mode, which corresponds to symmetric breathing of the RuH_6 octahedra, is the stiffest mode, and the next lower mode also involves modulation of the Ru—H bond lengths. The two intermediate modes (738 and 777 cm^{-1}) involve distortion of the octahedra, which would also yield lower frequency modes in oxides. The two lowest frequency modes are motions of the Sr atoms within their cages. The lowest mode is the antisym-

TABLE II. Calculated frequences ω (cm^{-1}) and displacement patterns for zone-center modes of Sr_2RuH_6, $a=14.361a_0$ compatible with $R32$ symmetry. The displacements are $(\alpha_{Sr},\alpha_{Sr},\alpha_{Sr})$ for the first Sr (in $R32$ symmetry), $(\beta_{Sr},\beta_{Sr},\beta_{Sr})$ for the second Sr, $(\gamma_{Ru},\gamma_{Ru},\gamma_{Ru})$ for Ru, $(\delta_{H_1},\varepsilon_{H_1},\varepsilon_{H_1})$ for the first type (in $R32$ symmetry) of H (three atoms), and $(\delta_{H_2},\varepsilon_{H_2},\varepsilon_{H_2})$ for the second type of H (three atoms). The δ_H are Ru—H bond stretch coordinates, while ε_H are Ru—H bond shears.

ω	α_{Sr}	β_{Sr}	γ_{Ru}	δ_{H_1}	ε_{H_1}	δ_{H_2}	ε_{H_2}
126	0.073	−0.078	0.002	0.001	0.013	0.002	−0.009
141	−0.051	−0.045	0.075	0.075	0.037	0.071	0.041
738	0.003	−0.000	−0.005	−0.024	−0.673	−0.079	0.195
777	−0.002	−0.003	−0.011	−0.087	0.188	−0.012	0.670
1433	0.000	0.000	0.015	−0.632	−0.055	−0.750	−0.020
1742	0.000	0.000	0.002	−0.757	0.012	0.643	−0.044

metric motion of the Sr, which is not ferroelectric. The frequencies of these Sr motions are compatible with the frequencies of the shearing modes that modulate Sr—H distances when the mass difference is accounted for.

This pattern of phonon modes is quite different from what would occur in an oxide near ferroelectricity. In that case, there would be a low frequency cooperative mode. This would consist of a distortion where the cations move relative to the O atoms comprising the octahedra, reflecting the high polarizability of the octahedra softened by covalent interactions.[34,35] Here, the mode corresponding to motion of the Ru with respect to the H is at high frequency (1433 cm^{-1}) and the lower frequency Sr derived modes have only a small component of Ru motion relative to the H octahedra.

V. ENERGETICS AND ZERO POINT EFFECTS

In order to better understand the stability of these compounds, we performed calculations of the formation enthalpies by comparison of the total energies with those of decomposition products. Specifically, we did calculations for the elements, Mg, Sr, Ca, Fe, Ru, and Os in their bulk metallic form (in the LDA at the experimental lattice parameters, parallel to the calculations done for the hydrides, including ferromagnetism for Fe), the H_2 molecule (relaxed, in the LDA) and MgH_2, CaH_2, and SrH_2 (using experimental lattice constants, but relaxed atomic positions). In addition calculations were done for elemental Be and the intermetallic phase Be_2Fe, which is the expected decomposition product of the hypothetical phase Be_2FeH_6 (see below).

For the H_2 molecule we used a cubic supercell of lattice parameter 4.5 Å. This yielded an LDA energy of −2.288 Ry, bond length of 0.765 Å, and bond stretching vibrational frequency of 4217 cm^{-1}. These results are in good agreement with previous LDA calculations, for example, Patton and coworkers report a vibrational frequency of 4188 cm^{-1} and bond length of 0.765 Å.[22] The H_2 zero point energy obtained from the LDA frequency is 25.2 kJ/mol. This is a substantial number, which underscores the fact[23–25] that zero point effects need to be considered in the thermodynamics of hydride formation. Here, we neglect metal modes, and consider only the H contribution to the zero point energies, which we write as $3\hbar\overline{\omega}$ per H_2 unit, where $\overline{\omega}$ is an average H vibrational frequency. The effective $\overline{\omega}$ for H_2 is 703 cm^{-1}, so for hydrides with $\overline{\omega} > 703$ cm^{-1}, zero point motion will reduce the formation energy, and the corresponding deuterides and tritides will form more easily than the hydrides, while for materials with $\overline{\omega} < 703$ cm^{-1}, the converse will be true.[23] At least in principle, this difference can be used to obtain the average H frequency from experimental formation energies of hydrides and deuterides.

In order to estimate $\overline{\omega}$ for the compounds considered here, we performed LDA calculations for selected distortions and assumed that the H behaves in an Einstein-like way. In particular, for MgH_2, we displaced a single H in the unit cell (which contains four equivalent H atoms) along the three principal directions in its cage and averaged the resulting frequencies to obtain an average frequency (the principal directions relative to the lattice are $[1,\bar{1},0]$, [1,1,0] and [0,0,1]). For CaH_2 and SrH_2, we used the average of the four full symmetry Raman modes that are H derived (there are two other such modes associated with metal motion). For the K_2PtCl_6 structure hydrides, we used the average of the highest two Γ-point modes consistent with rhombohedral symmetry (the highest of these is the full symmetry Raman breathing mode) to obtain an effective *B*-site metal–H bond stretching force constant (which contributes 1/3 of the modes) and obtained the effective force constant for the other two thirds of the modes by averaging the two other H derived modes from the rhombohedral symmetry and the octahedral rotation mode. As a test, we also calculated an average Einstein frequency for Mg_2FeH_6 by displacing a single H (of the six in the unit cell) perpendicular to the Fe—H "bond," and along it, similar to the procedure that was followed for MgH_2. This yielded a shear frequency of 727 cm^{-1} and a stretch frequency of 1828 cm^{-1}, for an average $\overline{\omega} = 1094$ cm^{-1}, in fortuitously good agreement with the estimate of 1089 cm^{-1}, made as above (Table III). In all cases, the averages are arithmetical averages of frequencies as is appropriate for the zero point energy.

α-MgH_2 has a tetragonal structure (space-group $P4_2/mmm$) with one H coordinate, x. We obtain $x=0.3046$, in agreeement with the recent neutron measurement of Bortz and co-workers,[26] who obtained $x=0.3040$, and an LDA calculation by Yu and Lam,[27] who also obtained $x=0.304$. Mov-

TABLE III. LDA energies in $\mathrm{kJ\,mol^{-1}}$ of formation on a per H_2 basis, assuming full decomposition into separated elemental metals and H_2 (minus means that the formation is exothermic). $\Delta H_{\mathrm{static}}$ denotes the LDA energy with no correction for zero point motion, $\overline{\omega}$ is the average phonon frequency estimated from LDA calculations and ΔH(LDA) is the zero-point corrected formation energy for the hydride. The LDA vibrational frequency of H_2 is used in this calculation. Experimental values are given as ΔH(expt).

Compound	$\Delta H_{\mathrm{static}}$	$\overline{\omega}(\mathrm{cm^{-1}})$	ΔH(LDA)	ΔH(expt)
Mg_2FeH_6	−147	1089	−133	−77, −86, −98
Ca_2FeH_6	−221	1033	−209	
Sr_2FeH_6	−211	871	−205	
Mg_2RuH_6	−147	968	−137	
Ca_2RuH_6	−229	1013	−218	
Sr_2RuH_6	−221	1006	−210	
Sr_2OsH_6	−216	1023	−205	
MgH_2	−90	954	−81	−75
CaH_2	−219	767	−217	−184
SrH_2	−207	670	−208	−180

ing a single hydrogen in the unit cell of MgH_2, we obtained frequencies of $1277\ \mathrm{cm^{-1}}$ along [1,1,0] (bond stretching) $592\ \mathrm{cm^{-1}}$ along $[1,\overline{1},0]$ (bond bending) and $993\ \mathrm{cm^{-1}}$ along [0,0,1] (mixed). The bond stretching "Einstein" frequency is near that of the full symmetry Raman mode, which we obtain at $1301\ \mathrm{cm^{-1}}$ and which is also of bond stretching character. This supports the simple Einstein-like approach used.

Good agreement with neutron diffraction results[28,29] is also obtained for the internal structural parameters of CaH_2 and SrH_2, which occur in an orthorhombic *Pnma* structure, as given in Table IV. As mentioned, the full symmetry Raman frequencies obtained from this relaxation, were used to construct the H frequency for the zero point contribution to the enthalpy of these compounds.

LDA formation energies are given in Table III. The formation energies of MgH_2, CaH_2, and SrH_2 are in reasonable agreement with the experiment (thermodynamic values are −75, −184, and −180 kJ/mol H_2, respectively[30]) and in good agreement with previous LDA calculations.[31,32] The values indicate overbinding of the hydride phases by 5–35 kJ/mol H_2, i.e., about 10%–20%. The formation energy of Mg_2FeH_6 is the best studied of the K_2PtCl_6 hydrides, and is reported as −98 kJ/mol (Ref. 2), −86 kJ/mol (Ref. 7), and −77.4 kJ/mol (Ref. 8). The calculated LDA energy of −133 kJ/mol is significantly larger and this difference would seem to be at the high end of the expected range of LDA errors, especially considering the reasonable agreement with experiment for MgH_2, and for FeAl, where we obtain agreement with experiment to within 5 kJ/mol of Fe.[33] Perhaps the largest errors come from spurious LDA self-interaction effects associated with H.[37,38] Besides LDA static binding energy errors, the most likely source of error is the crude method that we used to obtain an average phonon frequency. However, even if the average phonon frequency were $250\ \mathrm{cm^{-1}}$ higher than our estimate, which we think is unlikely, the calculated enthalpy would shift by only 9 kJ/mol of H_2.

One possibility is that some of the difference is experimental in origin, related to the possible existence of some stable hydride among the decomposition products, which would then stabilize the products relative to Mg_2FeH_6 and therefore would lower the formation energy as measured by the decomposition. In any case, we do find certain trends. First, Mg_2FeH_6 is by far the least stable of the K_2PtCl_6 hydrides studied. However, this is connected with the fact that MgH_2 is much less stable than SrH_2 or CaH_2. If one considers formation via $2DH_2+H_2+M\rightarrow D_2MH_6$, then this heat of formation is largest for Mg_2FeH_6 as might be expected from an ionic picture. Second, the formation energy per H_2 is significantly larger for Mg_2FeH_6 than for MgH_2. This implies that under thermodynamic conditions, without some very unusual entropy contribution, the decomposition should proceed directly to H_2 and the elements, or, at a bare minimum, if there is an intermediate hydride phase, it should not be MgH_2. The formation energies of the Ca and Sr compounds on the other hand are very close to those of CaH_2 and SrH_2, so depending on the conditions, those decompositions may very well proceed via an intermediate $M+DH_2$.

Similar calculations were done for the other compounds in order to estimate the H zero point energy, but these were at a lower level of convergence in the fitting of the dynamical matrix.

VI. STABILITY, BONDING, AND IMPLICATIONS

We now speculate about possible implications of our results for hydrogen storage. First, we note that the cohesion is ionic, and that it is the Madelung field that stabilizes the $[MH_6]^{4-}$ units. Changes in the Coulomb potential then ought

TABLE IV. LDA and experimental atomic positions [x(LDA), z(LDA) and x(exp), z(exp) for *Pnma* CaH_2 and SrH_2. $y=1/4$ for all atoms in this structure.

	x(LDA)	z(LDA)	x(exp)	z(exp)	Ref.
CaH_2 Ca	0.2380	0.1100	0.2378	0.1071	28
CaH_2 H1	0.3566	0.4274	0.3573	0.4269	28
CaH_2 H2	0.9741	0.6773	0.9737	0.6766	28
SrH_2 Sr	0.2382	0.1109	0.2438	0.1108	29
SrH_2 H1	0.3558	0.4278	0.3570	0.4281	29
SrH_2 H2	0.9732	0.6787	0.9693	0.6825	29

to strongly affect the bond lengths in these units as well as their stability. This is already apparent in the values of x_H of Table I, which show substantial changes in the M—H bond lengths as the lattice parameter is changed by D site substitution (note that the octahedra are not connected so that they need not breath with the lattice). This implies significant tunability in the properties with substitutions. Second, the ionic stabilization of the lattice implies that mixed M cation substitutions should be possible and that the octahedral coordination of the metal atoms will be preserved in them. For example, if the partial or full substution $Os \rightarrow \frac{1}{2}Re + \frac{1}{2}Ir$ could be made, its structure is expected to feature ReH_6 and IrH_6 octahedra, rather than different Re—H and Ir—H coordinations on this lattice. However, it is unclear if any of these substitutions can be made, and even if they can it is unclear whether they will be beneficial. Finally, we note that the fully hydrided compound can therefore be destabilized by driving the transition metal d states up in energy via the Madelung potential, if all other things were equal. One way would be to substitute some fraction of the Mg with a monovalent cation if one can be made to enter the lattice.

However, the stability is relative to the decomposed products, and it is clear from the calculated energetics that these play a major role. For example, Mg_2RuH_6 and Mg_2FeH_6 are the least stable compounds relative to decomposition into elemental Mg and Ru or Fe, but they are the most stable with respect to a hypothetical intermediate MgH_2+Fe/Ru. As mentioned, this suggests that under normal conditions Mg_2FeH_6 and Mg_2RuH_6 decompose into H_2 and elemental metals without any MgH_2 intermediate, consistent with the observation of Bogdanovic and co-workers.[8]

VII. REDUCING THE FORMATION ENERGY: HYPOTHETICAL Be_2FeH_6

Considering the trend in the energetics with respect to the alkaline earth element, one possibility for obtaining a lower formation energy would seem to be replacement of Mg by Be.[39] This would seem especially likely considering the properties of Be metal, which include strong bonding that would compete with the formation of hydride phases. In order to check this trend we performed calculations for hypothetical Be_2FeH_6 to obtain its formation energy. Since the compound is hypothetical, we obtained the lattice parameter by relaxation in the LDA. The calculated structure has a lattice parameter of 5.65 Å, a H internal coordinate of $x = 0.2648$, and a corresponding full symmetry Raman phonon frequency of 2233 cm^{-1}. No doubt the LDA underestimates the lattice parameter slightly, as is typical. In any case, with the LDA structure, we obtain a static formation enthalpy of −37 kJ/mol H_2 with respect to elemental products. This confirms the conjecture that Be would lead to lower binding energies. However, while this energy suggests that Be_2FeH_6 would be an interesting hydride phase, it neglects the fact that unlike Mg, Be forms compounds with Fe. In particular, $FeBe_2$ is a known intermetallic compound and would compete with the hydride phase. We calculated the enthalpy of formation of $FeBe_2$ (details are in the next section) and find −87 kJ/mol. The relevant energy for the stability of the hydride Be_2FeH_6 is therefore not the formation enthalpy from the elements, but from the intermetallic, $FeBe_2$, which, with H_2, would be the product of the decomposition. Relative to decomposition into the elements, the existence of the intermetallic then results in a shift of the formation enthalpy of Be_2FeH_6 by 29 kJ/mol on a per H_2 basis, to yield −8 kJ/mol. The average phonon frequency, determined as for the other K_2PtCl_6 hydrides, discussed above, is 1172 cm^{-1}, yielding a zero point correction of +17 kJ/mol H_2, placing the calculated enthalpy including zero point at +9 kJ/mol. Thus, it is likely that Be_2FeH_6 is marginally unstable with respect to decomposition into $FeBe_2$, and therefore will only be formed under high pressure or by chemical routes, if it can be made at all.

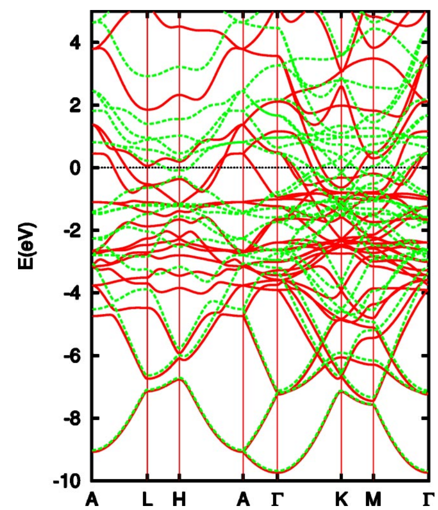

FIG. 7. (Color online) Band structure of ferromagnetic $FeBe_2$. Majority (minority) spin bands are given by solid red (dashed green) lines. The Fermi energy is at 0 eV.

VIII. ELECTRONIC STRUCTURE AND MAGNETISM IN $FeBe_2$

$FeBe_2$ is an interesting hard magnetic material. In particular, it has a relatively low density, high anisotropy, and a very high Curie temperature, T_C of 880 K.[40–42] Experimentally, $FeBe_2$ crystallizes in the hexagonal $MgZn_2$ structure (spacegroup $P6_3/mmc$, No. 194) and has magnetization, $M \approx 1.95\mu_B$/Fe. Since we are not aware of previous first principles studies of this material, we briefly summarize our results for the electronic structure of this compound.

The reported lattice parameters are $a = 4.215$ Å and $c = 6.853$ Å.[40] The unit cell contains four formula units. The Be atoms are on sites $2a$ (0,0,0) and $6h$ $(x, 2x, 1/4)$, while the Fe atoms are on $4f$ $(1/3, 2/3, z)$. Experimental values of the two internal parameters are not available, so they were found by structural relaxation in the LDA. We find $x = 0.8294$ and $z = 0.061$. The calculated LDA spin magnetization is $1.76\mu_B$/Fe and the magnetic energy is 0.237 eV/Fe. This is only $\sim 3kT_C$ suggesting some itinerant character.

The local spin density approximation (LSDA) band structure and density of states are given in Figs. 7 and 8. The band structure shows narrow crystal field split Fe $3d$ bands on top of a broad manifold of free electron like Be *sp* derived bands. These Be derived bands are weakly polarized, opposite to the Fe polarization, similar to the case of YFe_2, for example.[43,44] The majority spin Fe 3*d* bands are fully occupied, while the Fermi energy falls in the crystal field gap between the t_{2g} and e_g manifolds in the minority spin. This yields two minority spin e_g holes per Fe, and explains the $\sim 2\ \mu_B/\mathrm{Fe}$ magnetization. Relative to bcc Fe, there is a transfer of Fe *s* character to the Be derived bands, and a back transfer of charge to give effectively neutral Fe, with eight 3*d* electrons. This is consistent with the image discussed by Jesser and Vincze based on experimental susceptibility and Mossbauer measurements.[41] This pseudogapped band structure yields a relatively low density of states at the Fermi energy in both spin channels, $N_\uparrow(E_F) = 0.39\ \mathrm{eV}^{-1}$ and $N_\downarrow(E_F) = 0.67\ \mathrm{eV}^{-1}$ on a per formula unit basis.

The calculated formation energy of $FeBe_2$ is −87 kJ/mol on a per formula unit basis. As a test of our approach, we also calculated the formation energy of FeAl in the same way. The result was −77 kJ/mol(FeAl), which is in good agreement with the experimental value of −72.6 kJ/mol.[33,45] This suggests that the error in the formation energy of $FeBe_2$ is likely in the range of 5 kJ/mol.

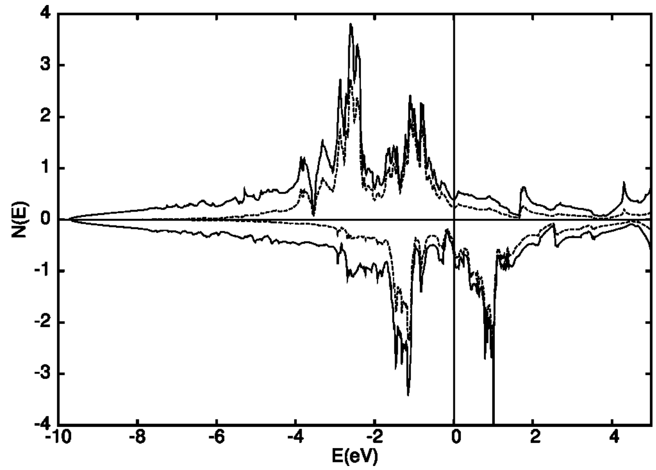

FIG. 8. Electronic density of states (solid) and Fe *d* projection onto the LAPW sphere (broken, radius 2.1 a_0) for $FeBe_2$ on a per per formula unit basis. Spin-up is above the 0 and spin down is shown as negative. The Fermi level is at 0 eV.

IX. FERROELECTRICITY AND HYPOTHETICAL Pb_2RuH_6 AND Be_2FeH_6

We did phonon calculations for the hypothetical compound Pb_2RuH_6. In perovskite and double perovskite oxides, Pb typically can be substituted for Sr. The Pb compounds typically have unit cell volumes very close to the Sr analogs, but are more likely to be ferroelectric because of Pb—O covalency (e.g., $PbTiO_3$ vs $SrTiO_3$). Since the experimental lattice parameter of Pb_2RuH_6 is unavailable, we used the value for Sr_2RuH_6. This choice also makes comparison of the two systems more direct. LDA relaxation of the lattice parameter yielded a value 1.8% smaller than this, but considering the usual underestimate of lattice parameters in the LDA, we do not consider the LDA value to be more reliable than the use of the Sr_2RuH_6 value.[36] The Pb_2RuH_6 modes (Table V) are qualitatively like those of Sr_2RuH_6, except that the low frequency Pb modes are shifted down in frequency. This shift is, however, larger than can be accounted for by the mass difference, and the modes are reversed in order. The lowest mode is now the symmetric mode and it is at zero frequency to within the precision of the present calculations. We also calculated the energy as a function of the rotation of the RuH_6 octahedron. Such rotational degrees of freedom compete with ferroelectricity in ferroelectrics such as $Pb(Zr,Ti)O_3$.[46] Here, these modes are stable. We obtain frequencies of 576 and 490 cm^{-1}, for Sr_2RuH_6 and Pb_2RuH_6 respectively.

We found a similar result for hypothetical Be_2FeH_6, which, however, might be a more difficult synthesis target. In this case, we obtained a slightly unstable mode of Be character, with a ferroelectric displacement pattern, and stable rotational and antiferroelectric modes. Significantly the ferroelectric mode is at 93*i* cm^{-1}, while the antiferroelectric Be mode is at 72 cm^{-1}. Taking into account the mass ratio of Pb and Be this shows a similar difference in the curvature of the energy surfaces of the ferroelectric and antiferroelectric *A*-site cation modes for Pb_2RuH_6 and Be_2FeH_6. However, since we used the LDA lattice parameter for Be_2FeH_6, which is expected to be an underestimate, perhaps by 1–2%, and since ferroelectricity is normally disfavored by compression,[46–48] Be_2FeH_6 may be the better candidate for ferroelectricity. As in Pb_2RuH_6, the octahedral rotational mode of Be_2FeH_6 is stable now at 541 cm^{-1}. The full symmetry Raman mode is calculated to be 2233 cm^{-1}. This suggests Pb_2RuH_6 and Be_2FeH_6 as a candidate ferroelectric hydrides. If these compounds are made, the possibility of

TABLE V. Phonon frequencies and displacement patterns, as in Table IV but for Pb_2RuH_6, $a = 14.361 a_0$; frequencies, ω are in cm^{-1}.

ω	α_{Pb}	β_{Pb}	γ_{Ru}	δ_{H_1}	$\varepsilon_{\mathrm{H}_1}$	δ_{H_2}	$\varepsilon_{\mathrm{H}_2}$
23	−0.023	−0.019	0.089	0.082	0.038	0.077	0.045
52	0.049	−0.048	0.005	0.005	0.025	0.004	−0.017
552	−0.002	−0.002	−0.010	−0.062	0.518	−0.013	0.469
632	0.002	−0.002	−0.001	−0.022	−0.473	0.041	0.520
1265	0.000	0.000	0.013	−0.646	−0.028	−0.745	−0.008
1626	−0.000	0.000	0.002	−0.749	0.002	0.654	−0.040

ferroelectricity should be investigated, e.g., by low temperature structural studies and temperature dependent dielectric measurements.

X. SUMMARY AND DISCUSSION

The present density functional calculations show that the K_2PtCl_6 hydrides are ionic compounds, with some covalency. The 18 electron rule is a consequence of ligand field effects on the transition metal site. This type of ionic character suggests the possibility of ferroelectricity in related hydrides. We find that the hypothetical compounds, Pb_2RuH_6 and Be_2FeH_6 are on the borderline of ferroelectricity, and should be investigated in this context, if they can be made. Furthermore, the ionic character stabilizes H anions, and Fe cations, which is why Fe participates in hydride formation, although Fe metal is not a hydride former. The ionic character implies a certain degree of tunability of the properties of these hydrides, which may allow adjustment of the thermodynamics. However, since Fe and Mg do not form intermetallic compounds, it is likely that the properties of Mg_2FeH_6 cannot be made better for vehicular H storage than those of MgH_2, since MgH_2 will be a competing phase.

One way to reduce the stability of the hydride without facing this limitation would be to focus on the stability of decomposition products. One possibility would be to explore minor additions, X that are soluble in and stabilize an Fe—Mg—X intermetallic. These need not enter the hydride lattice, provided that they are available, e.g., on hydride particle surfaces to promote the decomposition and provide sufficient enthalpy via the formation of the intermetallic. This may be the most promising avenue for modifying Mg_2FeH_6 for hydrogen storage applications; the solubility of Mg in $FeBe_2$ is not known. However, if Fe—Be—Mg intermetallics are stable, the present results suggest that the addition of Be to Mg_2FeH_6 may lead to lower stability, which if not for the toxicity of Be, would be favorable for applications.

ACKNOWLEDGMENTS

The authors are grateful for helpful discussions with P. Dantzer, M.R. Pederson, and K. Yvon. D.J.S thanks the University of Paris-Sud for their hospitality, which made this work possible. We also thank the Institut du Developpement et des Resources en Informatique Scientifique (IDRIS) for a grant of computer time. Work at the Naval Research Laboratory is supported by ONR.

*Present address: Condensed Matter Sciences Division, Oak Ridge National Laboratory, Oak Ridge, TN 37831–6032.

[1] R. O. Moyer, Jr., C. Stanitski, J. Tanaka, M. I. Kay, and B. Kleinberg, J. Solid State Chem. **3**, 541 (1971).

[2] J.-J. Didisheim, P. Zolliker, K. Yvon, P. Fischer, J. Schefer, M. Gubbelmann, and A. F. Williams, Inorg. Chem. **23**, 1953 (1984).

[3] M. Kritikos, D. Noreus, B. Bogdanovic, and U. Wilczok, J. Less-Common Met. **161**, 337 (1990).

[4] B. Huang, F. Bonhomme, P. Selvam, K. Yvon, and P. Fischer, J. Less-Common Met. **171**, 301 (1991).

[5] K. Yvon, Chimia **52**, 613 (1998).

[6] R. O. Moyer, Jr., R. Lindsay, and D. F. Storey, Z. Phys. Chem., Neue Folge **165**, 83 (1989).

[7] I. G. Konstanchuk, E. Yu. Ivanov, M. Pezat, B. Darriet, V. V. Boldyrev, and P. Hagenmuller, J. Less-Common Met. **131**, 181 (1987).

[8] B. Bogdanovic, A. Reiser, K. Schlichte, B. Spliethoff, and B. Tesche, J. Alloys Compd. **345**, 77 (2002).

[9] G. J. Miller, H. Deng, and R. Hoffmann, Inorg. Chem. **33**, 1330 (1994).

[10] D. J. Singh, Phys. Rev. B **53**, 176 (1996).

[11] E. Orgaz and M. Gupta, J. Phys.: Condens. Matter **5**, 6697 (1993).

[12] D. J. Singh, *Planewaves Pseudopotentials and the LAPW Method* (Kluwer Academic, Boston, 1994).

[13] D. Singh, Phys. Rev. B **43**, 6388 (1991).

[14] S. F. Parker, K. P. J. Williams, M. Bortz, and K. Yvon, Inorg. Chem. **36**, 5128 (1997).

[15] L. F. Mattheiss, Phys. Rev. B **43**, 1863 (1991).

[16] The H atom has significant self-interaction errors within the LDA, especially the nonspin polarized version that is appropriate to compare with the charge density of these nonspin polarized hydrides. The fully spin polarized LDA H atom, which is a better description, would have 0.35 e inside the 1.1 a_0 sphere.

[17] A. Aguayo and D. J. Singh, Phys. Rev. B **69**, 155103 (2004).

[18] A tetrahedral crystal field might also be thought to be favorable as it is also a geometry that is favorable for large large ligand field splittings and hybridization, but in that case only up to 12 electrons would be accommodated −8 in the 4 H 1s orbitals and 4 in the now lower e_g manifold. However, this is not compatible with the electron count of Fe and Mg.

[19] O. Gunnarsson, J. Phys. F: Met. Phys. **6**, 587 (1976).

[20] H. Yamada, J. Inoue, K. Terao, S. Kanda, and M. Shimizu, J. Phys. F: Met. Phys. **14**, 1943 (1984).

[21] I. I. Mazin and D. J. Singh, Phys. Rev. B **56**, 2556 (1997).

[22] D. C. Patton, D. V. Porezag, and M. R. Pederson, Phys. Rev. B **55**, 7454 (1997).

[23] E. Wicke and H. Brodowsky, in *Hydrogen in Metals II*, edited by G. Alefeld and J. Volkl (Springer, Berlin, 1978), pp. 73–155.

[24] H.-J. Tao, K.-M. Ho, and X.-Y. Zhu, Phys. Rev. B **34**, 8394 (1986).

[25] K. Miwa and A. Fukumoto, Phys. Rev. B **65**, 155114 (2002).

[26] M. Bortz, B. Bertheville, G. Bottger, and K. Yvon, J. Alloys Compd. **287**, L4 (1999).

[27] R. Yu and P. K. Lam, Phys. Rev. B **37**, 8730 (1988).

[28] A. F. Andresen, A. J. Maeland, and D. Slotfeldt-Ellingsen, J. Solid State Chem. **20**, 93 (1977).

[29] N. E. Brese, M. O'Keefe and R. B. von Dreele, J. Solid State Chem. **88**, 571 (1990).

[30] R. C. Weast, *Handbook of Chemistry and Physics, Sec. D* (CRC, New York, 1974).

[31] H. Smithson, C. A. Marianetti, D. Morgan, A. Van der Ven, A.

Predith, and G. Ceder, Phys. Rev. B **66**, 144107 (2002).
[32] C. Wolverton, V. Ozolins, and M. Asta, Phys. Rev. B **69**, 144109 (2004).
[33] One likely source of error is in the magnetic energy of elemental Fe, which is likely underestimated in the LDA. Generalized gradient approximation calculations give a correction of only ~5 kJ/mol of H_2; D. J. Singh, W. E. Pickett, and H. Krakauer, Phys. Rev. B **43**, 11628 (1991). The good agreement with experiment for the formation energy of FeAl (which is on the borderline of magnetism) from ferromagnetic Fe and Al supports the conclusion that the error due to the LDA treatment of the magnetic energy of Fe is small.
[34] R. E. Cohen, Nature (London) **358**, 136 (1992).
[35] D. J. Singh and L. L. Boyer, Ferroelectrics **136**, 95 (1992).
[36] The calculated LDA lattice parameters of Pb_2RuH_6 and Sr_2RuH_6 are 14.10 and 14.17 a_0, respectively, as compared to the experimental lattice parameter of 14.3619 a_0 for Sr_2RuH_6.
[37] T. Miyake, F. Aryasetiawan, H. Kino, and K. Terakura, Phys. Rev. B **61**, 16491 (2000).
[38] Z. Wu, R. E. Cohen, D. J. Singh, R. Gupta, and M. Gupta, Phys. Rev. B **69**, 085104 (2004).
[39] The trend with *A*-site cation is not surprising in an ionic picture. One can think of the formation energy in stages: first the formation of ions by atomization and ionization of the elements, and then formation of a lattice from the ions. The latter would favor smaller lattice parameters via the $1/r$ scaling of the Ewald energy (which is opposite to the calculated trends in the energies), but this is overcome by the large ionization and atomization energies. The sums of the experimental atomization, and first and second ionization energies for Be, Mg, Ca, and Sr are 2982, 2336, 1913, and 1778 kJ/mol, respectively; NIST.
[40] S. Jonsson, K. Kaltenbach, and G. Petzow, Z. Metallkd. **73**, 534 (1982).
[41] R. Jesser and I. Vincze, J. Phys. F: Met. Phys. **6**, 1567 (1976).
[42] H. Samata, Y. Nagata, S. Morita, G. Tanaka, T. Mitsuhashi, S. Yashiro, and S. Abe, J. Alloys Compd. **302**, 29 (2000).
[43] P. Mohn and K. Schwarz, Physica B & C **130**, 26 (1985).
[44] D. J. Singh and M. Gupta, Phys. Rev. B **69**, 132403 (2004).
[45] J. Breuer, A. Grun, F. Sommer, and E. J. Mittemeijer, Metall. Mater. Trans. B **32**, 913 (2001).
[46] M. Fornari and D. J. Singh, Phys. Rev. B **63**, 092101 (2001).
[47] G. A. Samara and A. A. Giardini, Phys. Rev. **A140**, 954 (1965); G. A. Samara, Phys. Rev. B **1**, 3777 (1970).
[48] D. J. Singh and L. L. Boyer, Ferroelectrics **136**, 95 (1992).